Published in final edited form as:
Exp Eye Res. 2010 September ; 91(3): 347–352. doi:10.1016/j.exer.2010.05.022.

Ocular pharmacokinetic study of a corticosteroid by ^{19}F MR

Xin Liu[a], **S. Kevin Li**[b], and **Eun-Kee Jeong**[c,*]

[a]Department of Physics and Astronomy, University of Utah, 115 South 400 East, Salt Lake City, UT 84112, USA

[b]Division of Pharmaceutical Sciences, College of Pharmacy, University of Cincinnati, 3225 Eden Ave, HPB 136, Cincinnati, OH 45267, USA

[c]Radiology, University of Utah, 729 Arapeen Drive, Salt Lake City, UT 84108, USA

Abstract

Traditional ocular pharmacokinetic studies are invasive and cannot be easily applied to humans *in vivo*. To acquire *in vivo* ocular pharmacokinetic data noninvasively, ^{19}F MR on a 3T clinical scanner was used to follow the real time dynamics of a corticosteroid in the eye. ^{1}H MR was also performed to locate the site of administration. Triamcinolone acetonide phosphate (TAP) was the model drug, administered by intravitreal and subconjunctival injections. TAP pharmacokinetics were monitored by changes in the ^{19}F spectrum of the intraocular drug in real time. The elimination half-lives of TAP in the eye after intravitreal and subconjunctival injections were 8 and 0.5 h *in vivo* and 17 and 6.0 h postmortem, respectively. The half-lives associated with clearance were 14 h for intravitreal injection and 0.5 h for subconjunctival injection.

Keywords

ocular pharmacokinetics; corticosteroid; TAP; ^{19}F MR

1. Introduction

Corticosteroids such as triamcinolone acetonide (TA) and dexamethasone sodium phosphate (DSP) have been widely used in the treatment of macular edema and uveitis (Kiernan and Mieler, 2009; Yilmaz et al., 2009). Intravitreal injection is an efficient way to deliver corticosteroid to the back of the eye to avoid systemic side effects. However, the intravitreal treatment is often short-lived, and repeated administration is usually required for chronic diseases (Kiernan and Mieler, 2009). Information on how long the drug will stay in the eye after the initial injection and the clearance of the drug after the injection is of significance that can help healthcare practitioners understand the duration of the therapeutic effect and modify the dosing regimen for effective therapy.

Conventional pharmacokinetics studies with animals require sacrificing the animals at different time points after drug administration, dissecting the eye, and analyzing different sections of the eye for the drug. The concentration of the drug in the eye tissues will then be determined using assays such as high-performance liquid chromatography (HPLC). However, this method is not applicable to humans. In human ocular pharmacokinetic studies, samples in the vitreous humor and anterior chamber could be extracted in conjunction with surgical procedures such as cataract surgery or vitrectomy (Cheng et al., 2009), but the amount of the drug in the eye or

*Corresponding author. Tel.: +1 801 581 8643; fax: +1 801 585 3592. ekj@ucair.med.utah.edu (E.-K. Jeong).

in eye tissues cannot be measured accurately and can only be estimated. The lack of human pharmacokinetic data in ocular drug delivery research has hindered its development and the advance of ocular drug delivery technologies. A noninvasive approach to study ocular pharmacokinetics and drug clearance in the eye, e.g., after intravitreal injections, does not only reduce the number of animals required in ocular drug delivery and pharmacokinetic research, but also allow the determination of the concentration profiles in the eye on a real time basis. Such methods may also be applicable to humans in clinical studies.

The objective of the present study was to develop a noninvasive way using ^{19}F MR on a 3T clinical scanner to study ocular pharmacokinetics of fluorine-containing therapeutic agents. Particularly, the real time pharmacokinetics of intraocular triamcinolone acetonide phosphate (TAP) was monitored after intravitreal injection using rabbits as the animal model *in vivo*. These results were compared with the pharmacokinetics of TAP after subconjunctival injection. Experiments were also conducted with the animals postmortem to evaluate the effect due to dynamic clearance. TAP is a prodrug of TA and has higher water solubility than TA (Fig. 1). The molecular weight of TAP is close to that of TA and DSP. Since the molecular structures of TAP and DSP are similar, the diffusion coefficient of TAP in the vitreous humor is expected to be similar to that of DSP, making TAP a useful surrogate to study the behavior of DSP clearance in the eye.

2. Materials and methods

2.1. Materials

TAP dipotassium salt was purchased from Crystal Pharma (Valladolid, Spain). TAP 0.09 M was prepared by dissolving TAP powder in deionized water. $MnCl_2$ tetrahydrate was obtained from Spectrum Chemical (Gardena, CA). Ethylenediamine tetraacetic acid (EDTA) and xylazine were acquired from Sigma Chemical (St. Louis, MO). $Na_2MnEDTA$ solutions (0.02 M) were prepared by mixing $MnCl_2$ with EDTA in deionized water and adjusting the pH of the solution to 7 with concentrated NaOH.

2.2. Animals

New Zealand white rabbits of 3–4 kg body-weight were purchased from Western Oregon Rabbit Co. (Philomath, OR). Animal experiments were conducted with the approval of the Institutional Animal Care and Use Committee at the University of Utah.

2.3. Animal experiments

Rabbits were anesthetized by intramuscular injection of 25–50 mg/kg ketamine and 5–10 mg/kg xylazine. The rabbits were then given either intravitreal or subconjunctival injections of 0.1 mL 0.09 M TAP mixed with approximately 1 μmol of $Na_2MnEDTA$ (MnEDTA ion). In postmortem rabbit studies, rabbits were sacrificed immediately before TAP injection. A total of 12 eyes were used for intravitreal injection: 6 eyes of 3 rabbits *in vivo* and 6 eyes of 3 rabbits postmortem; 6 eyes were used for subconjunctival injection: 3 eyes of 2 rabbits (the other eye was used for other purposes, e.g., a control) *in vivo* and 3 eyes of 2 rabbits postmortem. ^{19}F spectra were obtained at different time points after the injection. To determine the injection spot, MnEDTA ion was monitored with T_1-weighted ^{1}H imaging. ^{1}H MRI was taken before and at the time points after the injections.

2.4. MRI

All MRI experiments were performed on a Siemens 3T Trio clinical imaging system (Siemens Medical Solution, Erlangen, Germany). Because most of the clinical scanners do not have commercial ^{19}F coils and coil-to-scanner interface, a purpose-built circular linear surface coil

with 1.5 inch diameter was developed and tuned to 115.93 MHz to transmit the excitation pulse and receive the ^{19}F NMR signal. A similar coil with the same dimension was tuned to 123.22 MHz to acquire ^{1}H anatomy images. The coil assembly consisted of an RF resonator, Transmit/Receive (T/R) switch, preamplifier, and the coil-plug. In this experiment, surface coils were used to improve the signal detection sensitivity. The 1.5 inch diameter coil allowed the rabbit eye to slightly protrude out of the coil plane, which made the eyeball sit symmetrically about the coil plane. This was to position the eyeball in the most sensitive region of the coil. Since the surface coil field penetration depth was about same as the size as the coil, a coil diameter of 1.5 inches ensured that the sensitivity region of the coil covered deep enough for the eyeball. Active T/R switching with PIN diodes and a quarter-wave ($\lambda/4$) coaxial cable were used to switch between transmit and receive modes of the coil assembly. The same $\lambda/4$ was used for both proton and ^{19}F channels. A 3–200 MHz broadband preamplifier was used to amplify the received MR signals. A small vial of potassium fluoride (KF) solution was attached to the ^{19}F coil to generate a reference signal to calibrate the signal difference caused by coil loading variation.

A dynamic ^{19}F spectrum was obtained with a free induction decay (FID) pulse sequence: 1 s repetition time (TR), 0.15 ms receiver delay time, 16 kHz receiver bandwidth, 90° flip angle, 256 averages, and vector size of 1024. The data acquisition time was 4 min 20 s. A rectangular (hard) RF pulse was used with a 200 μs pulse width. The irradiation bandwidth (~10 kHz) covered both TAP and F^{-}ion peaks, which are separated by about 47 ppm (~5.4 kHz at the 3T). The NMR data were acquired at various time points after the intravitreal and subconjunctival injections as described in the “Animal Experiments” section. For some rabbits, multiple measurements were taken at the same time points.

High-resolution ^{1}H images were acquired using a gradient recall echo (GRE) pulse sequence: field of view (FOV) 108 mm, 50% phase-FOV, spatial resolution $0.34 \times 0.34 \times 1.5$ mm^3, 20 slices, TR 400 ms, echo time (TE) 4.28 ms, 400 Hz/pixel bandwidth, 2 averages, 60° flip angle, and acquisition time 2 min 10 s.

The T_1 of intravitreal TAP was also obtained during the experiment to determine if there was any T_1 change with decrease of TAP concentration. FID pulse sequences were used to acquire T_1-weighted spectra: 0.15 ms receiver delay time, 16 kHz bandwidth, 90° flip angle and 256 averages, repetition times were 200, 400, 800, 1600 and 3200 ms.

2.5. MR data processing

All ^{19}F spectra were processed by custom-programmed MR spectroscopy analysis software developed using IDL (Interactive Data Language, ITT Visual Software, Boulder, CO). 10 Hz Gaussian apodization was applied in the time domain, followed by baseline correction, Fourier-transformation, and phase-correction. The peak area integrations for both TAP and KF NMR lines were performed within the software. Ratios of the KF peak area to the TAP peak area at all time points were calculated then multiplied by TAP peak areas at each corresponding time point to create TAP signals with consistent coil sensitivity, i.e. normalized TAP signals. For each rabbit eye, the relative TAP signals were calculated as ratios of the normalized TAP signals at different time points to the normalized TAP signal at the initial time point.

3. Results

3.1. Intravitreal and subconjunctival injections

A typical ^{19}F spectrum of TAP and KF obtained from the present experiments is shown in Fig. 2a, the separation of two peaks is about 47 ppm, which is about 5.4 kHz on the 3T scanner. Fig. 2b shows the ^{19}F spectra of a representative rabbit eye *in vivo* at different time points after

intravitreal injection, where all spectra have been normalized to the KF spectrum. The data show the change in the spectrum over time throughout the experiment (from 0 to 22 h). The TAP peaks maintained similar shapes and widths while the height decreased over time to the level of noise after 22 h (the upper right spectrum). The signal-to-noise ratio (SNR) of the spectrum at the initial time point in the experiments ranged from 50 to 80.

The ^{1}H MR images of the same eye are shown in Fig. 3, immediately before, immediately after, and 5 h after the intravitreal injection. The MR images of MnEDTA show the site of the injection. The injection spot was close to the center of the vitreous body, and the solution immediately spread in both directions to the retina and the back of the lens. The images also show that the shape of the injection spot in the vitreous was not entirely spherical and MnEDTA spread behind the lens. The spreading suggests a less resistive region behind the lens to the flow of the solution introduced by the needle during the injection. At 5 h after the injection, MnEDTA had spread throughout the vitreous body and other parts of the eye. In addition to showing the location of the intravitreal injection, the MnEDTA data also provided information on the diffusion pattern of TAP since MnEDTA and TAP have similar molecular weights (~386 and 529 Da, respectively) and are expected to have similar diffusion coefficients.

Fig. 4 presents the amount of TAP at different time points after the intravitreal injection *in vivo* (6 eyes) and postmortem (6 eyes). Fig. 5 shows the amount of TAP at different time points after the subconjunctival injection *in vivo* (3 eyes) and postmortem (3 eyes). The data of each eye were fit into a first order clearance model to determine the elimination half-life ($t_{1/2}$) of the TAP signal in each experiment using the first order exponential function:

$$A = A_0 \times \exp(-k_{obs} t) \quad (1)$$

where A is the signal (proportional to the drug concentration), A_0 is the initial signal, k_{obs} is the rate constant, and t is time. The average elimination half-life $t_{1/2}$ was calculated and is presented in Table 1.

3.2. ^{19}F T_1 measurement of intraocular TAP

The MR signal intensity follows an exponential recovery equation:

$$S = S_0 \times [1 - \exp(-\mathrm{TR}/\mathrm{T}_1)] \quad (2)$$

where S and S_0 are the transient and the equilibrium signal intensities, respectively. With a fixed TR, T_1 change will affect the signal intensity. ^{19}F T_1 was measured as 907 ± 165 ms and 883 ± 370 ms at 20 min and 4 h after the intravitreal injection, respectively. The ^{19}F T_1 values of TAP were essentially the same that indicates negligible effect on the ^{19}F signal intensity during the experiment. In the subconjunctival injection experiments, the TAP signal decayed quickly and T_1 measurements were not performed.

4. Discussion

4.1. Ocular clearance

Drugs delivered through intravitreal injections can be eliminated through the aqueous humor outflow pathways in the anterior of the eye such as the canal of Schlemm or across the retinal/choroidal layer surrounding the vitreous (Maurice, 2001; Urtti, 2006). For small molecules, the predominant route of clearance is suggested to be through the retina in the posterior segment of the eye (Worakul and Robinson, 1997). The diffusion of a drug in the vitreous mainly depends on its molecular weight (or molecular size), and permeation across the retina depends

on the lipophilicity of the drug. Therefore, clearance from the vitreous, e.g., after intravitreal injections, generally depends on the molecular weight, lipophilicity, and charge of the molecule. These factors also determine if clearance is diffusion or barrier controlled. Small lipophilic molecules usually have faster clearance than charged molecules provided that binding to ocular tissues is not important. For example, the terminal half-lives of small molecules in the vitreous in rabbits can range from 3 to 4 h for the corticosteroid dexamethasone (Graham and Peyman, 1974; Kwak and D'Amico, 1992), to 5 h for the antibiotic carbenicillin (Barza et al., 1982) and to greater than 12 h for the antiviral foscarnet (Berthe et al., 1994). Whereas dexamethasone is lipophilic and uncharged having a molecular weight of 392 Da, carbenicillin and foscarnet are charged (2–, and 3–, respectively) with molecular weights of 378 and 126 Da, respectively. The half-life of third-generation cephalosporins in the vitreous humor ranges from 5 to 20 h (Barza et al., 1993). In the present study, TAP, a charged molecule of 515 Da, had a half-life of 8 h after intravitreal injection, which is consistent with the range provided in the literature. Clearance from the subconjunctival pocket and anterior chamber after subconjunctival injection is believed to be through the conjunctival vasculature and lymphatics (Lee and Robinson, 2001, 2004; Ghate et al., 2007) and the aqueous humor outflow pathways, respectively, and is generally fast compared with that from the vitreous. In general, the half-lives of molecules in the subconjunctival pocket are approximately 0.3–0.5 h after subconjunctival injection (Li et al., 2004; Kim et al., 2008). Half-lives of clearance from the anterior chamber are less than 1 h for pilocarpine (Lee and Robinson, 1982) and methazolamide (Maren and Jankowska, 1985) and up to 2 h for dorzolamide (Sugrue, 1996). The TAP result after subconjunctival injection in the present study is in the same order of magnitude as those in the literature. Clearance of intravitreal injection of drugs in suspension form is generally much slower than water soluble drugs. Half-life of triamcinolone acetonide clearance from vitreous, for example, is 5–6 days in rats (Oishi et al., 2008).

TAP can be a surrogate to study ocular pharmacokinetics of therapeutic agents of similar physiochemical properties (molecular size and charge) and understand the mechanism of clearance after intravitreal and subconjunctival injections. For example, TAP and DSP have similar molecular weights, and if the clearance is diffusion controlled after intravitreal administration, the behavior of TAP clearance will be similar to that of DSP.

4.2. Intravitreal and subconjunctival injections

The present results show that the TAP signal decays at a much higher rate after subconjunctival injection *in vivo* than after intravitreal injection *in vivo* (1.4 vs. 0.09 h^{-1}). This is consistent with the mechanisms of ocular clearance and the pharmacokinetic profiles observed after subconjunctival and intravitreal injections in the literature as described in the preceding section on ocular clearance. A major difference between the routes of ocular clearance after subconjunctival injection versus intravitreal injection *in vivo* is the distance for TAP to reach the clearance site such as the blood vasculature in the choroid and retina or to reach the anterior chamber and the Schlemm's canal. Following subconjunctival injection, TAP is in direct contact with the blood vasculature in the surrounding tissues of the subconjunctival space. Clearance of TAP after intravitreal injection, requires diffusion across the vitreous humor before it can be cleared from the eye.

4.3. In vivo and postmortem studies

If euthanasia compromised the tissue barriers in the eye, an increase in TAP clearance was expected postmortem. On the other hand, if clearance was the dominant factor, a decrease in TAP clearance was expected due to the lack of a functional vasculature around the eyes postmortem. The present data show significantly slower clearance of TAP from the eye in the postmortem animals compared with those *in vivo*: 0.04 vs. 0.09 h^{-1} for postmortem and *in vivo* after intravitreal injection, and 0.11 vs. 1.4 h^{-1} for postmortem and *in vivo* after

subconjunctival injection, respectively. This is consistent with blood circulation around the eyes being a dominant factor for the decrease in the TAP signal. Although the blood retina barrier (e.g., endothelial cell tight junctions) became compromised after animal death (Berkowitz et al., 2004), an assumption that the tissues in the eye such as the sclera, choroid, and retina remained structurally intact postmortem (Kim et al., 2004) was made as a first approximation in the pharmacokinetic analysis. Under this assumption, the effect of dynamic clearance such as clearance through the blood vasculature and lymph flow could be estimated by the following pharmacokinetic model:

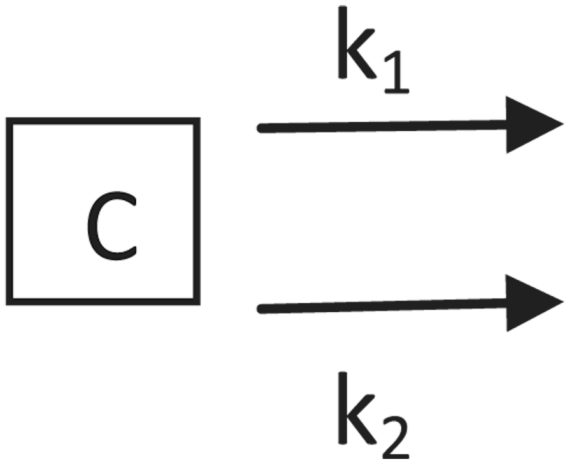

$$\frac{dC}{dt} = -(k_1 + k_2)C \tag{3}$$

where k_1 is the rate constant of TAP clearance from the eye due to blood vasculature and other factors that cease at the death of the animal and k_2 is the rate constant due to clearance such as passive diffusion and other factors in the animal postmortem. Accordingly, k_2 equals the rate constant of TAP observed postmortem and the sum $k_1 + k_2$ equals the apparent rate constant k_{obs} of clearance *in vivo*. A comparison of the *in vivo* and postmortem results shows that the rate constants k_1 for TAP (due to dynamic clearance, e.g., blood vasculature clearance) are 0.05 and 1.3 h^{-1} after intravitreal and subconjunctival administrations, respectively. This corresponds to the termination half-lives due to clearance of 14 h for intravitreal injection and 0.5 h for subconjunctival injection.

4.4. Other considerations

It has been suggested that the position of the intravitreal injection is important for drug distribution and elimination in the eye (Friedrich et al., 1997a, 1997b). For example, when the site of injection for intravitreal delivery is at the center of the vitreous body and the TAP solution injected maintains a spherical shape, TAP would diffuse isotropically and then be cleared by blood vasculature at the retina. This scenario would result in the slowest clearance due to the diffusion that needs to take place. However, as shown in Fig. 3 in the present study, MnEDTA had already reached the retina soon after the intravitreal injection. The problem is possibly caused by the relatively large amount of TAP solution (0.1 mL) injected, compared to the volume of the rabbit vitreous humor (0.7–1.5 mL). This would increase the clearance rate of TAP after the injection and introduce variability in intravitreal injection in general.

Other reasons that might contribute to the signal decrease include the degradation of TAP to TA in the eye, an inhomogeneous RF field distribution, and the change in T_1 of TAP in different eye compartments or by other factors such as partial pressure of oxygen. The first explanation

is based on the low solubility of TA in the vitreous humor; the aqueous solubility of TA is approximately 0.036 mg/mL (Wiedmann et al., 2000) although a previous study has shown that the aqueous concentration of TA in the vitreous is 0.2 mg/mL (Yang et al., 1998) possibly due to TA interactions with the vitreous humor components. TA in solid state is expected to have a short T_2 so the signal would decrease significantly when TAP is converted to TA and subsequently precipitated in the vitreous. However, this cannot explain the different results observed in the *in vivo* and postmortem experiments. The second explanation is related to coil signal inhomogeneity, in which TAP might diffuse to the places in the eye with less coil sensitivity. Again, if this were the major reason for the decrease in the TAP signal, the *in vivo* and postmortem experiments would not show different results. The last explanation was found to be unlikely because T_1 measurements have shown similar T_1 values (907 vs. 883 ms, respectively) at 20 min and 4 h after the injection.

It should be noted that the presence of MnEDTA should not affect the pharmacokinetics of TAP in the present study as the amount of MnEDTA injected and the concentration of the MnEDTA solution used in the experiments were low and unlikely to introduce severe acute toxicity. Mn ion has been used in MRI and show minimal toxicity at low concentration (Watanabe et al., 2001; Thuen et al., 2009) and the chelating ion EDTA is generally recognized as safe (GRAS). For example, a dose of 100–150 nmol Mn administrated as 0.05–1 M $MnCl_2$ solution intravitreally in rats, which corresponds to approximately 10 mM Mn when distributed equally throughout the rat eye, was suggested not to have toxic effects (Watanabe et al., 2001; Thuen et al., 2008).

4.5. Detection and limitations

There are limitations using rabbits as an animal model to study drug pharmacokinetics at the back of the eye and to extrapolate the results to human because the eyes such as the inner retinal blood circulations in rabbits and human are dissimilar. The goal of the present study is to eventual apply this technique on human in the future. To use ^{19}F MR to study ocular pharmacokinetics in human, some technical issues remain to be addressed. Particularly, the ^{19}F MR method has relatively low sensitivity compared to traditional assay techniques (e.g., HPLC and GC). The detection limit of ^{19}F MR for TAP was about 0.18 μmol with the current RF coil and setup. When the TAP amount was less than 0.18 μmol in the eye, the signal was below noise level (about 2% of the 9 μmol initial total amount of the TAP injected). Although the SNR of the spectrum at the initial time points was 50–80 and provided sufficient detection in the present intravitreal and subconjunctival injection study, this detection limit may not be sensitive enough for ocular pharmacokinetic studies to evaluate other ocular drug delivery methods. Further hardware improvement or pulse sequence modification is required to increase the detection limit.

5. Conclusion

A whole-body clinical MRI system was modified to perform ^{19}F MR with a FID pulse sequence for noninvasive ocular pharmacokinetic studies. Ocular pharmacokinetic experiments were conducted using triamcinolone acetonide phosphate (TAP) as the model drug in rabbits *in vivo* and postmortem. The apparent elimination rate constants and half-lives of TAP in the eye after drug administration were determined. The difference in clearance observed *in vivo* and postmortem suggests the importance of fluid dynamics in the eye and blood circulation around the eyes to TAP clearance. The rate constants related to such clearance were then calculated. The higher clearance after subconjunctival injection relative to that of intravitreal injection was believed to be due to the distance of the injection site from the blood vasculature. Finally, the present study demonstrates the feasibility of noninvasively monitoring the clearance of

fluorine-containing drugs after ocular delivery using ^{19}F MR, which may allow the eventual use of this method to study ocular pharmacokinetics in human.

Acknowledgments

This research was supported by NIH Grant EY15181. The authors thank Dr. Sarah A. Molokhia for her help in some experiments and Dr. Roy Rowley for his careful review of the wording and grammar in this paper.

References

Barza M, Kane A, Baum J. The effects of infection and probenecid on the transport of carbenicillin from the rabbit vitreous humor. Invest. Ophthalmol. Vis. Sci 1982;22:720–726. [PubMed: 7076417]

Barza M, Lynch E, Baum JL. Pharmacokinetics of newer cephalosporins after subconjunctival and intravitreal injection in rabbits. Arch. Ophthalmol 1993;111:121–125. [PubMed: 8424709]

Berkowitz BA, Roberts R, Luan H, Peysakhov J, Mao X, Thomas KA. Dynamic contrast-enhanced MRI measurements of passive permeability through blood retinal barrier in diabetic rats. Invest. Ophthalmol. Vis. Sci 2004;45:2391–2398. [PubMed: 15223822]

Berthe P, Baudouin C, Garraffo R, Hofmann P, Taburet AM, Lapalus P. Toxicologic and pharmacokinetic analysis of intravitreal injections of foscarnet, either alone or in combination with ganciclovir. Invest. Ophthalmol. Vis. Sci 1994;35:1038–1045. [PubMed: 8125715]

Cheng L, Banker AS, Martin M, Kozak I, Freeman WR. Triamcinolone acetonide concentration of aqueous humor after decanted 20-mg intravitreal injection. Ophthalmology 2009;116:1356–1359. [PubMed: 19450879]

Friedrich S, Cheng YL, Saville B. Drug distribution in the vitreous humor of the human eye: the effects of intravitreal injection position and volume. Curr. Eye Res 1997a;16:663–669. [PubMed: 9222083]

Friedrich S, Cheng YL, Saville B. Finite element modeling of drug distribution in the vitreous humor of the rabbit eye. Ann. Biomed. Eng 1997b;25:303–314. [PubMed: 9084836]

Ghate D, Brooks W, McCarey BE, Edelhauser HF. Pharmacokinetics of intraocular drug delivery by periocular injections using ocular fluorophotometry. Invest. Ophthalmol. Vis. Sci 2007;48:2230–2237. [PubMed: 17460284]

Graham RO, Peyman GA. Intravitreal injection of dexamethasone. Treatment of experimentally induced endophthalmitis. Arch. Ophthalmol 1974;92:149–154. [PubMed: 4211214]

Kiernan DF, Mieler WF. The use of intraocular corticosteroids. Expert Opin. Pharmacother 2009;10:2511–2525. [PubMed: 19761356]

Kim H, Robinson MR, Lizak MJ, Tansey G, Lutz RJ, Yuan P, Wang NS, Csaky KG. Controlled drug release from an ocular implant: an evaluation using dynamic three-dimensional magnetic resonance imaging. Invest. Ophthalmol. Vis. Sci 2004;45:2722–2731. [PubMed: 15277497]

Kim SH, Csaky KG, Wang NS, Lutz RJ. Drug elimination kinetics following subconjunctival injection using dynamic contrast-enhanced magnetic resonance imaging. Pharm. Res 2008;25:512–520. [PubMed: 17674155]

Kwak HW, D'Amico DJ. Evaluation of the retinal toxicity and pharmacokinetics of dexamethasone after intravitreal injection. Arch. Ophthalmol 1992;110:259–266. [PubMed: 1736876]

Lee TW, Robinson JR. Drug delivery to the posterior segment of the eye: some insights on the penetration pathways after subconjunctival injection. J. Ocul. Pharmacol. Ther 2001;17:565–572. [PubMed: 11777180]

Lee TW, Robinson JR. Drug delivery to the posterior segment of the eye II: development and validation of a simple pharmacokinetic model for subconjunctival injection. J. Ocul. Pharmacol. Ther 2004;20:43–53. [PubMed: 15006158]

Lee VHL, Robinson JR. Disposition of pilocarpine in the pigmented rabbit eye. Int. J. Pharm 1982;11:155–165.

Li SK, Molokhia SA, Jeong EK. Assessment of subconjunctival delivery with model ionic permeants and magnetic resonance imaging. Pharm. Res 2004;21:2175–2184. [PubMed: 15648248]

Maren TH, Jankowska L. Ocular pharmacology of sulfonamides: the cornea as barrier and depot. Curr. Eye Res 1985;4:399–408. [PubMed: 4017632]

Maurice D. Review: practical issues in intravitreal drug delivery. J. Ocul. Pharmacol. Ther 2001;17:393–401. [PubMed: 11572470]

Oishi M, Maeda S, Hashida N, Ohguro N, Tano Y, Kurokawa N. Pharmacokinetic behavior of intravitreal triamcinolone acetonide prepared by a hospital pharmacy. Jpn. J. Ophthalmol 2008;52:489–492. [PubMed: 19089571]

Sugrue MF. The preclinical pharmacology of dorzolamide hydrochloride, a topical carbonic anhydrase inhibitor. J. Ocul. Pharmacol. Ther 1996;12:363–376. [PubMed: 8875343]

Thuen M, Berry M, Pedersen TB, Goa PE, Summerfield M, Haraldseth O, Sandvig A, Brekken C. Manganese-enhanced MRI of the rat visual pathway: acute neural toxicity, contrast enhancement, axon resolution, axonal transport, and clearance of Mn(2+). J. Magn. Reson. Imaging 2008;28:855–865. [PubMed: 18821627]

Thuen M, Olsen O, Berry M, Pedersen TB, Kristoffersen A, Haraldseth O, Sandvig A, Brekken C. Combination of Mn(2+)-enhanced and diffusion tensor MR imaging gives complementary information about injury and regeneration in the adult rat optic nerve. J. Magn. Reson. Imaging 2009;29:39–51. [PubMed: 19097077]

Urtti A. Challenges and obstacles of ocular pharmacokinetics and drug delivery. Adv. Drug Deliv. Rev 2006;58:1131–1135. [PubMed: 17097758]

Watanabe T, Michaelis T, Frahm J. Mapping of retinal projections in the living rat using high-resolution 3D gradient-echo MRI with Mn2+-induced contrast. Magn. Reson. Med 2001;46:424–429. [PubMed: 11550231]

Wiedmann TS, Bhatia R, Wattenberg LW. Drug solubilization in lung surfactant. J. Control. Release 2000;65:43–47. [PubMed: 10699268]

Worakul N, Robinson JR. Ocular pharmacokinetics/pharmacodynamics. Eur. J. Pharm. Biopharm 1997;44:71–83.

Yang CS, Khawly JA, Hainsworth DP, Chen SN, Ashton P, Guo H, Jaffe GJ. An intravitreal sustained-release triamcinolone and 5-fluorouracil codrug in the treatment of experimental proliferative vitreoretinopathy. Arch. Ophthalmol 1998;116:69–77. [PubMed: 9445210]

Yilmaz T, Weaver CD, Gallagher MJ, Cordero-Coma M, Cervantes-Castaneda RA, Klisovic D, Lavaque AJ, Larson RJ. Intravitreal triamcinolone acetonide injection for treatment of refractory diabetic macular edema: a systematic review. Ophthalmology 2009;116:902–911. quiz 912–903. [PubMed: 19410949]

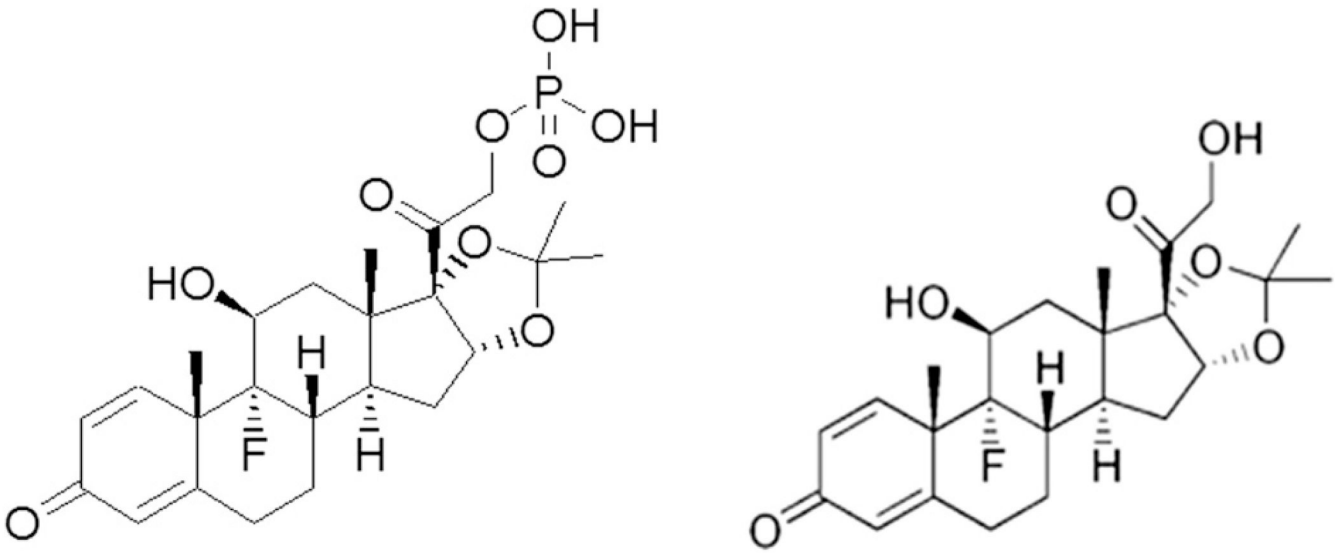

Fig. 1.
Molecular structures of triamcinolone acetonide phosphate (left) and triamcinolone acetonide (right).

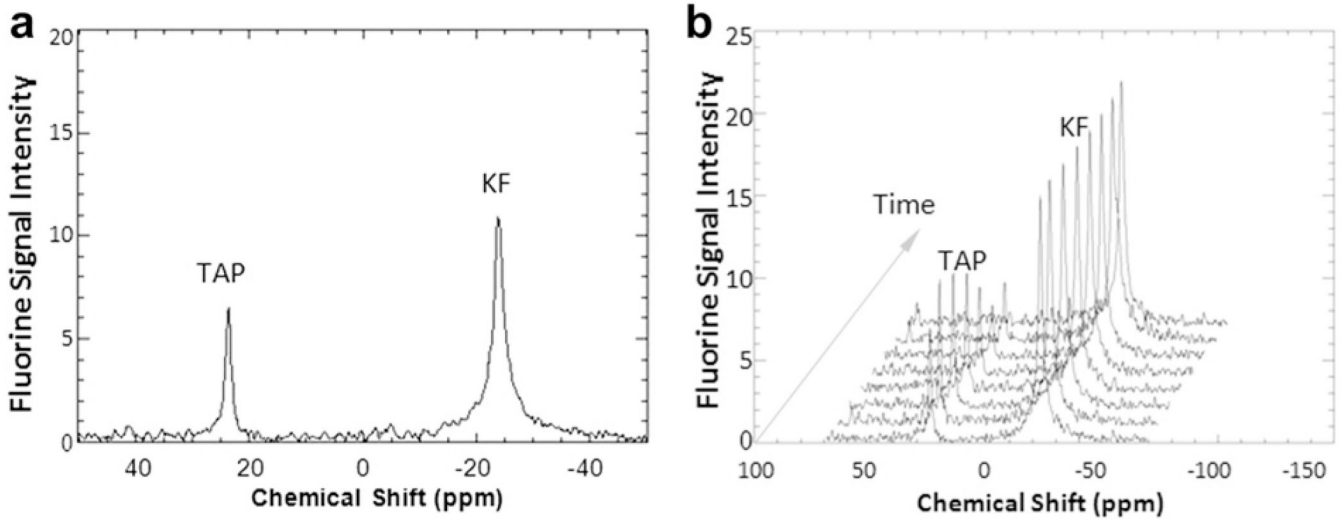

Fig. 2.

Representative ^{19}F spectra at (a) one time point and (b) different time points obtained in a rabbit *in vivo*, where all spectra have been normalized according to the KF spectrum. In (b), the time axis is not spaced according to the time scale.

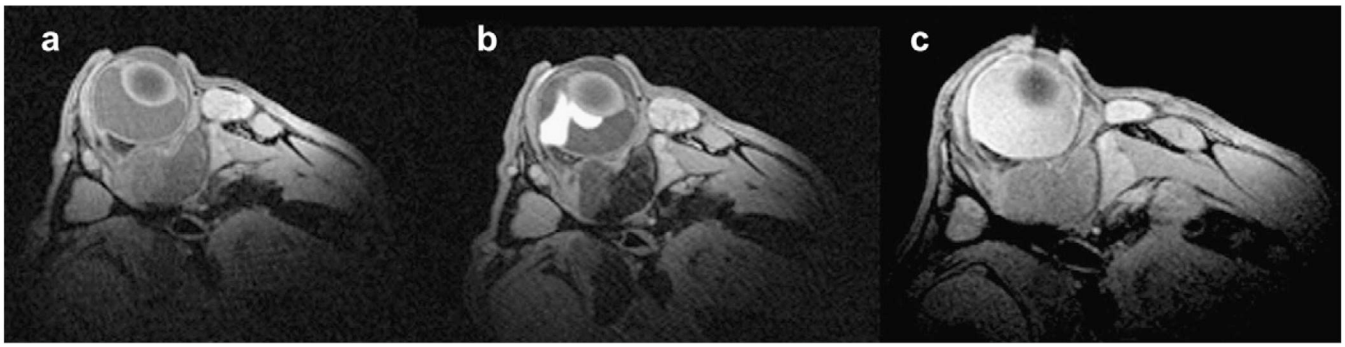

Fig. 3.
^{1}H MR images (a) right before, (b) immediately and (c) 5 h after the intravitreal injection. The bright region in (b) indicates the initial location of the TAP/MnEDTA/saline solution.

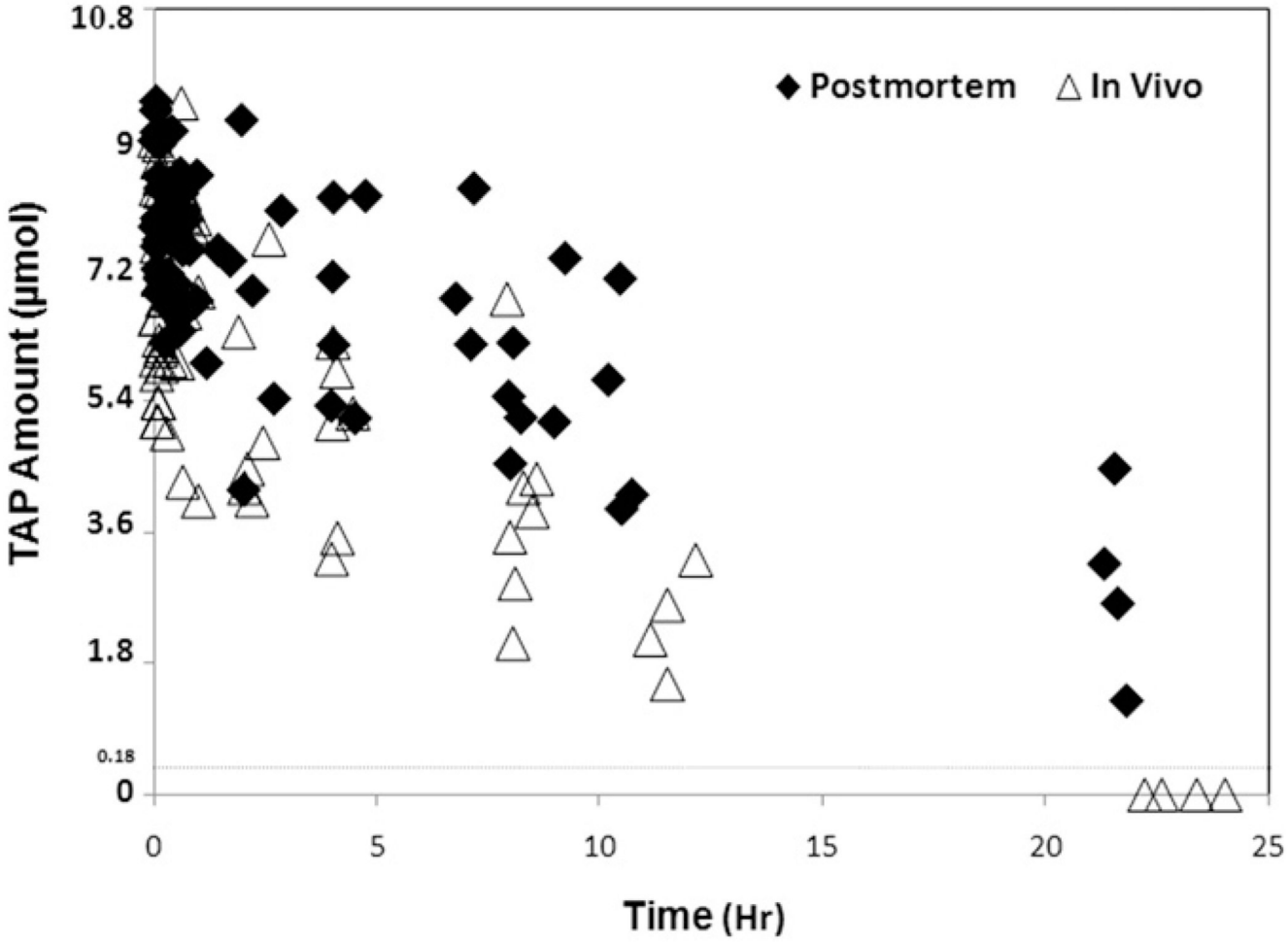

Fig. 4.

Amount of TAP determined from TAP signal versus time after intravitreal injection *in vivo* and postmortem. The dotted line indicates the detection limit with the coil and pulse sequence used in this study.

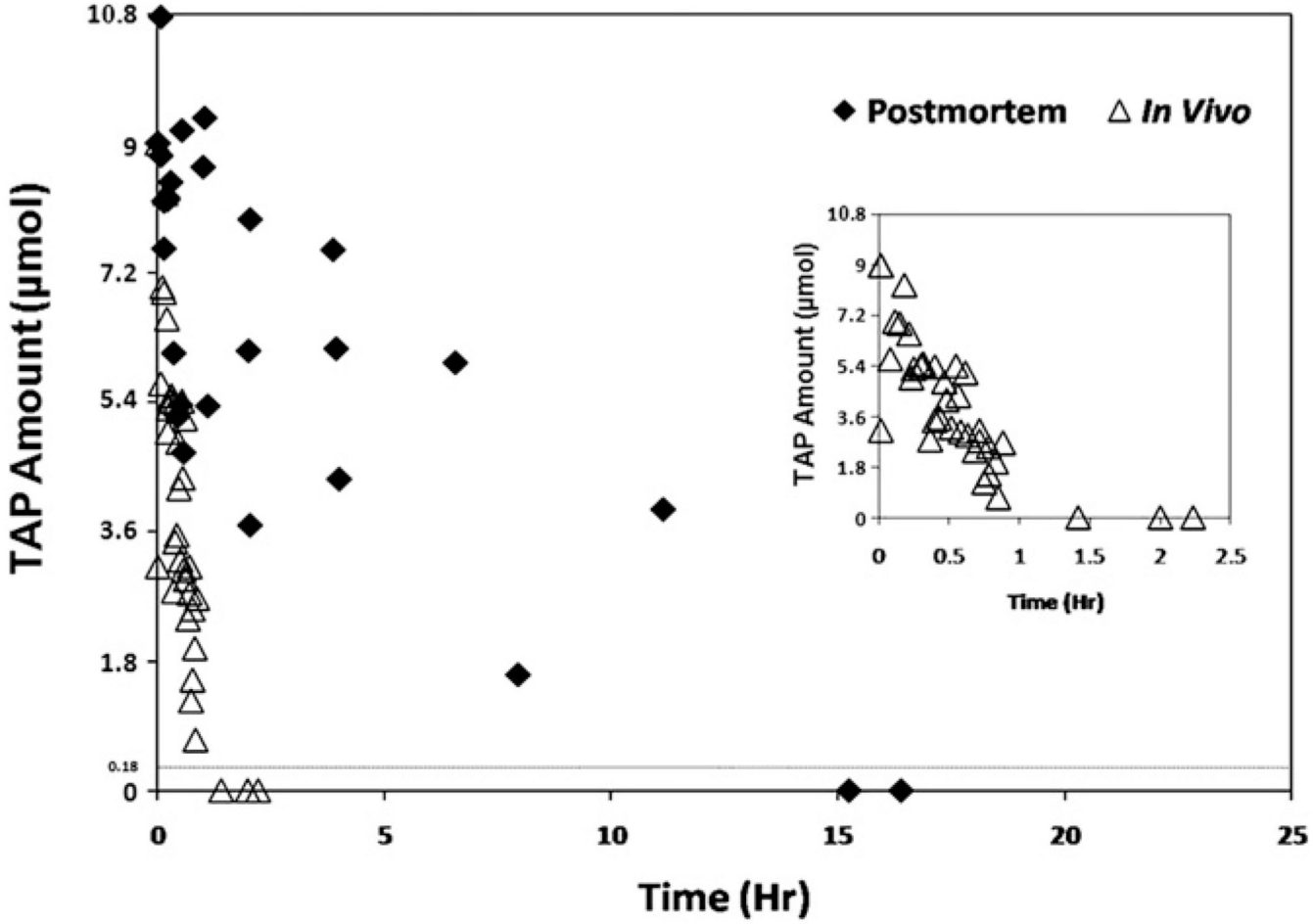

Fig. 5.

Amount of TAP determined from TAP signal versus time after subconjunctival injection *in vivo* and postmortem. The insert shows an enlarged view of the early *in vivo* data. The dotted line indicates the detection limit with the coil and pulse sequence used in this study.

Table 1

Summary of the first order rate constant and elimination half-life.[a].

	k_{obs} (h^{-1})	$t_{1/2}$ (h)
Intravitreal injection *in vivo*	0.09 ± 0.02	7.8 ± 1.1
Intravitreal injection postmortem	0.04 ± 0.01	17.2 ± 2.1
Subconjunctival injection *in vivo*	1.4 ± 0.2	0.5 ± 0.1
Subconjunctival injection postmortem	0.11 ± 0.03	6.0 ± 1.5

[a]Mean ± SD (n = 3 for subconjunctival injection; n = 6 for intravitreal injection).